11th World Congress on Computational Mechanics (WCCM XI)
5th European Conference on Computational Mechanics (ECCM V)
6th European Conference on Computational Fluid Dynamics (ECFD VI)
E. Oñate, J. Oliver and A. Huerta (Eds)

SIMPLIFIED MODEL FOR STRUCTURAL VIBRATION OF A VIADUCT DUE TO RAILWAY TRAFFIC

Y. F. CHEN[*] AND T. X. WU[*]

[*] School of Mechanical Engineering, Shanghai Jiao Tong University
Shanghai 200240, P R China
e-mail: txwu@sjtu.edu.cn

Key Words: *Structural Vibration, Elevated Railway, Viaduct, Beam, Dynamic Stiffness Matrix method.*

Abstract. For estimation of the dynamic performance of the concrete viaduct structure in the metropolitan light rail systems and design of measures for reducing its structure-born noise, the finite element (FE) method is usually time-consuming, because of large size of the structure and large frequency range covered for analysis. In this paper, a simplified 2.5D model is developed for quick prediction of the frequency response of a U-section viaduct. A longitudinal beam model is used to simulate the vibration of the viaduct along the track, and a multi-beam frame model to simulate the dynamic properties of the cross section of the viaduct. The vibrational energy of the viaduct calculated from the 2.5D model approximates to that from the FE model, while the computational cost is much lower. This model can effectively be used for quick prediction of the dynamic performances of viaduct structures and design of noise control measures.

1 INTRODUCTION

Concrete viaduct structures are used for the elevated lines in metropolitan light rail systems. Although its construction is easier and costs less than the underground tunnel, the sound radiated from the viaduct structure during the train passage causes environmental noise problem. It is therefore necessary to design effective measures for reducing the structure-born noise from the viaduct [1].

Before implementation of the noise control measures designed, their performance should be estimated by numerical simulation or physical test. In terms of simulation, FE softwares such as ANSYS are usually used for vibration analysis. Wu and Liu [2] compared the structural vibration and sound emission of two kinds of concrete viaduct, the box-section and U-section structure, by numerical simulation and in-situ measurements, and FE models of two kinds of viaducts are used for the numerical simulation. Li and Wu [3] obtained the vibrational power flows within a coupled vehicle-track-bridge system, in which models of a real urban U-section bridge are built using two- or three- dimensional finite elements.

However, as the viaduct is a large structure and the analysis frequencies can be up to hundreds Hertz, the calculations using FE models are very time-consuming in most situation. Especially in the design stage, different parameters should be optimized in the calculations in order to find cost-effective results, and thus it is important to develop a simplified and effective model for the dynamic simulations.

In this work a simplified 2.5D model is developed for calculation of the vibrational energy of a U-section viaduct during the train passage. Theoretical solutions can be obtained using an Euler-Bernoulli Beam model and a multi-beam frame model.

2 SIMPLIFIED 2.5D MODEL OF U-SECTION VIADUCT

A simplified model is developed for dynamic analysis of a U-section viaduct structure, which is composed of a bottom plate and two side plates and has symmetry of shape, as shown in Fig. 1(a). The railway track is laid on the bottom plate of the structure and the viaduct is supported by two piers at its ends.

In the simplified model two kinds of beam model are used to represent the dynamic properties of the viaduct. One is a longitudinal beam to simulate the vibration modes of the viaduct along the track, and the other is a multi-beam frame to simulate the dynamic properties of the cross section of the viaduct. To combine these two models, the viaduct is divided into several sections along its longitudinal direction firstly. And the vertical displacement of the mid-point of every section, which can be treated as the average displacement of this section, is obtained by using the longitudinal beam model. Then, the displacements distribution of the section can be obtained by analyzing displacement response of the multi-beam frame model under a unit concentrated force. Multiplying the displacement response distribution of the multi-beam frame model by an enlarging coefficient simultaneously to make the average displacement of certain section equal to the displacement of the longitudinal beam model at this section, the displacement distribution all over the viaduct is acquired.

With regard to the longitudinal beam model, viaduct between two piers can be simplified into one simply supported beam under uniformed harmonic excitation, as the piers at both ends can be viewed as simply supports. According to the classical Euler-Bernoulli theory, the displacement response of the model can be easily written as follow.

$$v(x,t)=\sum_{n=1,3,5}^{\infty}\frac{4q}{\rho An\pi}\frac{1}{\omega_n^2-\omega^2}\sin\frac{n\pi x}{L}e^{i\omega t},\quad \omega_n=\left(\frac{n\pi}{L}\right)^2\sqrt{\frac{EI}{\rho A}} \tag{1}$$

where E, ρ, A, and I represent the Young's modulus, density, cross sectional area and inertia moment of the cross section of the beam, respectively. L is the length of the viaduct between two neighboring piers; q is intensity of pressure acting on unit length of the beam; and ω_n is the natural frequency corresponding to the nth vibration mode of the beam.

As for the multi-beam frame model, two straight beams are respectively used to simulate the bottom plate and one of the side plates of the viaduct, and a lumped mass is added onto the top of the side beam representing as the rib of the side wall, which is shown in Fig. 1(b). A concentrated harmonic excitation is acting on the viaduct through the rail and no displacement constraint is added on the model. Analytical solution of the response of the model can be determined by dynamic stiffness matrix method. The detailed procedures of the method are described below.

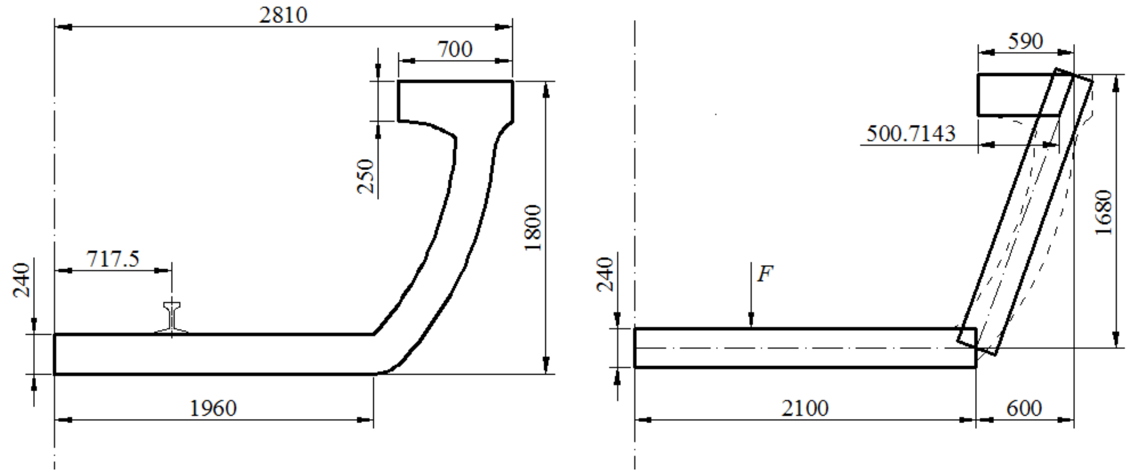

(a) **(b)**

Figure 1: Section geometry of (a) the viaduct; (b) the simplified multi-beam frame model.

3 VIBRATION OF MULTI-BEAM FRAME MODEL USING DYNAMIC STIFFNESS MATRIX METHOD

3.1 Dynamic stiffness matrix of a single beam

The differential equations of motion for the longitudinal and flexural vibrations of a beam are respectively given by

$$-EA\frac{\partial^2 u}{\partial x^2}+\rho A\frac{\partial^2 u}{\partial t^2}=0\,, \tag{2}$$

$$EI\frac{\partial^4 v}{\partial x^4}+\rho A\frac{\partial^2 v}{\partial t^2}=0\,, \tag{3}$$

where the displacement components u and v are illustrated in Fig. 2. Assuming $u(x, t) = U(x)e^{i\omega t}$ and $v(x, t) = V(x)e^{i\omega t}$, the solution of the model shape $U(x)$ and $V(x)$ are

$$U(x)=C_1\cos k_x x+C_2\sin k_x x\,, \tag{4}$$
$$V(x)=C_3\sin k_y x+C_4\cos k_y x+C_5\sinh k_y x+C_6\cosh k_y x\,.$$

where $k_x=\omega\sqrt{\rho/E}$ and $k_y=\sqrt[4]{\rho A/EI}\bullet\sqrt{\omega}$ are wave numbers of longitudinal and flexural wave, respectively.

Fig. 2 also shows the rotation angle, forces and moments of the beam, where $\theta(x, t) = \Theta(x)e^{i\omega t}$ is the rotation angle, $N^0(x, t) = N(x)e^{i\omega t}$ is the longitudinal force, $Q^0(x, t) = Q(x)e^{i\omega t}$ is the shearing force, and $M^0(x, t) = M(x)e^{i\omega t}$ is the bending moment. For the sign convention used in Fig. 2, they are given by

$$\Theta=\frac{\partial V}{\partial x},\quad N=EA\frac{\partial U}{\partial x},\quad Q=EI\frac{\partial^3 V}{\partial x^3},\quad M=EI\frac{\partial^2 V}{\partial x^2}\,. \tag{5}$$

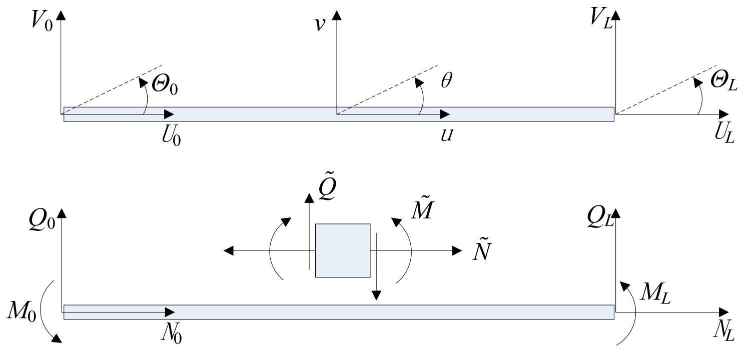

Figure 2: Displacements and forces of a single beam.

The displacement and force components at both ends of the beam can then be determined by substituting Eq. (4) into (5) and setting $x = 0$ and L, respectively. For a beam numbered i in a multi-beam frame model, its displacement and force components can be written as

$$\mathbf{D}^{(i)} = \begin{Bmatrix} \mathbf{D}_0^{(i)} \\ \mathbf{D}_L^{(i)} \end{Bmatrix} = \mathbf{P}^{(i)}\mathbf{C}^{(i)}, \quad \mathbf{F}^{(i)} = \begin{Bmatrix} \mathbf{F}_0^{(i)} \\ \mathbf{F}_L^{(i)} \end{Bmatrix} = \mathbf{Q}^{(i)}\mathbf{C}^{(i)}, \tag{6}$$

where

$$\mathbf{D}_0^{(i)} = \left\{ U_0^{(i)} \quad V_0^{(i)} \quad \Theta_0^{(i)} \right\}^T = \left\{ U^{(i)}(0) \quad V^{(i)}(0) \quad \Theta^{(i)}(0) \right\}^T,$$
$$\mathbf{D}_L^{(i)} = \left\{ U_L^{(i)} \quad V_L^{(i)} \quad \Theta_L^{(i)} \right\}^T = \left\{ U^{(i)}(L) \quad V^{(i)}(L) \quad \Theta^{(i)}(L) \right\}^T,$$
$$\mathbf{F}_0^{(i)} = \left\{ N_0^{(i)} \quad Q_0^{(i)} \quad M_0^{(i)} \right\}^T = \left\{ -N^{(i)}(0) \quad Q^{(i)}(0) \quad -M^{(i)}(0) \right\}^T,$$
$$\mathbf{F}_L^{(i)} = \left\{ N_L^{(i)} \quad Q_L^{(i)} \quad M_L^{(i)} \right\}^T = \left\{ N^{(i)}(L) \quad -Q^{(i)}(L) \quad M^{(i)}(L) \right\}^T,$$
$$\mathbf{C}^{(i)} = \left\{ C_1 \quad C_2 \quad C_3 \quad C_4 \quad C_5 \quad C_6 \right\}^T.$$

The relationship between the force and displacement components, according to Eq. (6), can be derived.

$$\begin{Bmatrix} \mathbf{F}_0^{(i)} \\ \mathbf{F}_L^{(i)} \end{Bmatrix} = \begin{bmatrix} \mathbf{K}_{00}^{(i)} & \mathbf{K}_{0L}^{(i)} \\ \mathbf{K}_{L0}^{(i)} & \mathbf{K}_{LL}^{(i)} \end{bmatrix} \begin{Bmatrix} \mathbf{D}_0^{(i)} \\ \mathbf{D}_L^{(i)} \end{Bmatrix}, \quad OR \;\; \mathbf{F}^{(i)} = \mathbf{K}^{(i)}\mathbf{D}^{(i)}, \;\; \mathbf{K}^{(i)} = \mathbf{Q}^{(i)}\left[\mathbf{P}^{(i)}\right]^{-1}, \tag{7}$$

where the matrix $\mathbf{K}^{(i)}$ is the dynamic stiffness matrix of beam i.

3.2 Dynamic stiffness matrix of a single beam with lumped mass at the ends

Now consider a single beam with lumped mass at its two ends, assuming that the masses and the moments of inertia of the lumped masses at the end of $x = 0$ and $x = \mathrm{L}$ are m_0, m_L, J_0 and J_L, respectively. Fig. 3 shows the internal and external force components at the ends of the beam. The continuity equations between the beam and two lumped masses can be written as

$$(N_0 - N_a)e^{i\omega t} = m_0 \frac{\partial^2 u(0,t)}{\partial t^2} = -m_0\omega^2 U_0 e^{i\omega t}, \qquad (N_L - N_a)e^{i\omega t} = m_L \frac{\partial^2 u(L,t)}{\partial t^2} = -m_L\omega^2 U_L e^{i\omega t}, \tag{8}$$

$$(Q_0 - Q_a)e^{i\omega t} = m_0 \frac{\partial^2 v(0,t)}{\partial t^2} = -m_0\omega^2 V_0 e^{i\omega t}, \qquad (Q_L - Q_a)e^{i\omega t} = m_L \frac{\partial^2 v(L,t)}{\partial t^2} = -m_L\omega^2 V_L e^{i\omega t},$$
$$(M_0 - M_a)e^{i\omega t} = J_0 \frac{\partial^2 \theta(0,t)}{\partial t^2} = -J_0\omega^2 \Theta_0 e^{i\omega t}, \qquad (M_L - M_a)e^{i\omega t} = J_L \frac{\partial^2 \theta(L,t)}{\partial t^2} = -J_L\omega^2 \Theta_L e^{i\omega t}.$$

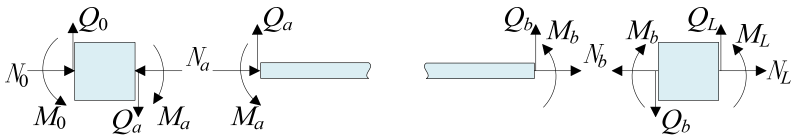

Figure 3: Displacements and forces of a single beam and lumped masses on its ends.

For the beam i in a multi-beam frame model, Eq. (8) can be rewritten as

$$\mathbf{F}^{(i)} - \mathbf{F}_{in}^{(i)} = -\omega^2 \mathbf{M}\mathbf{D}^{(i)}, \tag{9}$$

where **F** and **D** have the same meanings as in Eq. (6), and

$$\mathbf{F}_{in}^{(i)} = \{N_a \quad Q_a \quad M_a \quad N_b \quad Q_b \quad M_b\}^T, \quad \mathbf{M} = diag(m_0, m_0, J_0, m_L, m_L, J_L).$$

The internal force components, according to Eq. (7), is given by $\mathbf{F}_{in}^{(i)} = \mathbf{K}^{(i)}\mathbf{D}^{(i)}$, Thus, Eq. (9) can be rewritten as

$$\mathbf{F} = \left[\mathbf{K} - \omega^2\mathbf{M}\right]\mathbf{D}, \quad OR \quad \begin{Bmatrix} \mathbf{F}_0 \\ \mathbf{F}_L \end{Bmatrix} = \begin{bmatrix} \mathbf{K}_{00} - \omega^2\mathbf{M}_0 & \mathbf{K}_{0L} \\ \mathbf{K}_{L0} & \mathbf{K}_{LL} - \omega^2\mathbf{M}_L \end{bmatrix} \begin{Bmatrix} \mathbf{D}_0 \\ \mathbf{D}_L \end{Bmatrix}, \tag{10}$$

where $\mathbf{M}_0$ = diag(m_0, m_0, J_0), $\mathbf{M}_L$ = diag(m_L, m_L, J_L). And the matrix [$\mathbf{K}-\omega^2\mathbf{M}$] is the dynamic stiffness matrix of beam i with lumped masses at both of its ends.

3.3 Dynamic stiffness matrix of the multi-beam frame model of the viaduct

The multi-beam frame model, representing a half of the cross section of the viaduct, is composed of three beams and a lumped mass, as shown in Fig. 4. Assuming that the displacement components in the global Cartesian coordinate system at the four nodes, or the ends of the three beams, are respectively D_{xj}, D_{yj}, and Θ_{xyj}, and the force components are respectively F_{xj}, F_{yj}, and M_{xyj}, j = 1, 2, 3, 4. The relationship between the displacement components in the global coordinate system and the ones in the local coordinate system of beams are given by

$$\begin{Bmatrix} \mathbf{D}_1 \\ \mathbf{D}_2 \end{Bmatrix} = \begin{Bmatrix} \mathbf{D}_0^{(1)} \\ \mathbf{D}_L^{(1)} \end{Bmatrix}, \quad \begin{Bmatrix} \mathbf{D}_2 \\ \mathbf{D}_3 \end{Bmatrix} = \begin{Bmatrix} \mathbf{D}_0^{(2)} \\ \mathbf{D}_L^{(2)} \end{Bmatrix}, \quad \begin{Bmatrix} \mathbf{D}_3 \\ \mathbf{D}_4 \end{Bmatrix} = \begin{bmatrix} \mathbf{T}^{(3)} & \\ & \mathbf{T}^{(3)} \end{bmatrix} \begin{Bmatrix} \mathbf{D}_0^{(3)} \\ \mathbf{D}_L^{(3)} \end{Bmatrix}, \tag{11}$$

where $\mathbf{D}_i = \{D_{xi}, D_{yi}, \Theta_{xyi}\}^T$, and $\mathbf{T}^{(3)}$ is the coordinate transformation matrix of beam 3, which is given by

$$\mathbf{T}^{(3)} = \begin{bmatrix} \cos\varphi & -\sin\varphi & 0 \\ \sin\varphi & \cos\varphi & 0 \\ 0 & 0 & 1 \end{bmatrix}, \tag{12}$$

where φ is the angle between beam 3 and the x axis in the global coordinate system. The force components in two coordinate systems have the similar relationship as Eq. (11).

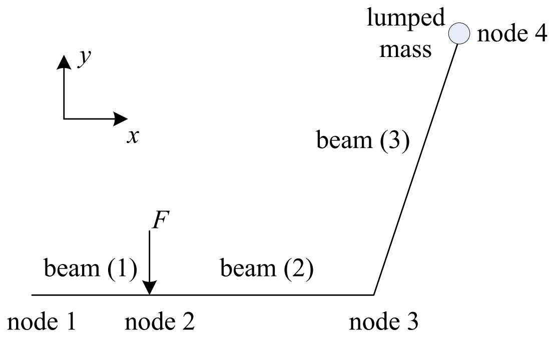

Figure 4: Beams and the lumped mass of the multi-beam frame model.

The relationships between the force and displacement components in global coordinate system at the ends of beams (1) and (2), according to Eqs. (7) and (11), are given by

$$\begin{Bmatrix} \mathbf{F}_1 \\ \mathbf{F}_2 \end{Bmatrix} = \begin{bmatrix} \mathbf{K}_{00}^{(1)} & \mathbf{K}_{0L}^{(1)} \\ \mathbf{K}_{L0}^{(1)} & \mathbf{K}_{LL}^{(1)} \end{bmatrix} \begin{Bmatrix} \mathbf{D}_1 \\ \mathbf{D}_2 \end{Bmatrix}, \quad \begin{Bmatrix} \mathbf{F}_2 \\ \mathbf{F}_3 \end{Bmatrix} = \begin{bmatrix} \mathbf{K}_{00}^{(2)} & \mathbf{K}_{0L}^{(2)} \\ \mathbf{K}_{L0}^{(2)} & \mathbf{K}_{LL}^{(2)} \end{bmatrix} \begin{Bmatrix} \mathbf{D}_2 \\ \mathbf{D}_3 \end{Bmatrix}. \tag{13}$$

As for nodes at the ends of beam (3), according to Eqs. (10) and (11), the relationship equation can be written as

$$\begin{Bmatrix} \mathbf{F}_3 \\ \mathbf{F}_4 \end{Bmatrix} = \begin{bmatrix} \mathbf{T}^{(3)} & \\ & \mathbf{T}^{(3)} \end{bmatrix} \begin{bmatrix} \mathbf{K}_{00}^{(3)} & \mathbf{K}_{0L}^{(3)} \\ \mathbf{K}_{L0}^{(3)} & \mathbf{K}_{LL}^{(3)} - \omega^2 \mathbf{M} \end{bmatrix} \begin{bmatrix} \mathbf{T}^{(3)} & \\ & \mathbf{T}^{(3)} \end{bmatrix}^{-1} \begin{Bmatrix} \mathbf{D}_3 \\ \mathbf{D}_4 \end{Bmatrix} = \begin{bmatrix} \bar{\mathbf{K}}_{00}^{(3)} & \bar{\mathbf{K}}_{0L}^{(3)} \\ \bar{\mathbf{K}}_{L0}^{(3)} & \bar{\mathbf{K}}_{LL}^{(3)} \end{bmatrix} \begin{Bmatrix} \mathbf{D}_3 \\ \mathbf{D}_4 \end{Bmatrix}, \tag{14}$$

$$\bar{\mathbf{K}}_{00}^{(3)} = \mathbf{T}^{(3)} \mathbf{K}_{00}^{(3)} \left[\mathbf{T}^{(3)} \right]^{-1}, \ \bar{\mathbf{K}}_{0L}^{(3)} = \mathbf{T}^{(3)} \mathbf{K}_{0L}^{(3)} \left[\mathbf{T}^{(3)} \right]^{-1},$$

$$\bar{\mathbf{K}}_{L0}^{(3)} = \mathbf{T}^{(3)} \mathbf{K}_{L0}^{(3)} \left[\mathbf{T}^{(3)} \right]^{-1}, \ \bar{\mathbf{K}}_{LL}^{(3)} = \mathbf{T}^{(3)} \left[\mathbf{K}_{LL}^{(3)} - \omega^2 \mathbf{M} \right] \left[\mathbf{T}^{(3)} \right]^{-1}.$$

where $\mathbf{M} = \mathrm{diag}(m, m, J)$, m and J are the mass and moment of inertia of the lumped mass, respectively.

Thus, the relationship between force and displacement components at nodes of the multi-frame beam model in global coordinate system is given by

$$\begin{Bmatrix} \mathbf{F}_1 \\ \mathbf{F}_2 \\ \mathbf{F}_3 \\ \mathbf{F}_4 \end{Bmatrix} = \begin{bmatrix} \mathbf{K}_{00}^{(1)} & \mathbf{K}_{0L}^{(1)} & & \\ \mathbf{K}_{L0}^{(1)} & \mathbf{K}_{LL}^{(1)} + \mathbf{K}_{00}^{(2)} & \mathbf{K}_{0L}^{(2)} & \\ & \mathbf{K}_{L0}^{(2)} & \mathbf{K}_{LL}^{(2)} + \bar{\mathbf{K}}_{00}^{(3)} & \bar{\mathbf{K}}_{0L}^{(3)} \\ & & \bar{\mathbf{K}}_{L0}^{(3)} & \bar{\mathbf{K}}_{LL}^{(3)} \end{bmatrix} \begin{Bmatrix} \mathbf{D}_1 \\ \mathbf{D}_2 \\ \mathbf{D}_3 \\ \mathbf{D}_4 \end{Bmatrix}, \ OR \ \mathbf{F}^g = \mathbf{K}^g \mathbf{D}^g, \tag{15}$$

where the matrix $\mathbf{K}^g$ is the dynamic stiffness matrix of the multi-frame beam model.

The boundary conditions of the model are: a symmetry displacement constraint on node 1 and a force in y direction imposed on node 2, i.e.,

$$D_{x1} = 0, \Theta_{xy1} = 0, \tag{16}$$

$$\begin{Bmatrix} F_{y1} & F_{x2} & F_{y2} & M_{xy2} & F_{x3} & F_{y3} & M_{xy3} & F_{x4} & F_{y4} & M_{xy4} \end{Bmatrix}^T = \begin{Bmatrix} 0 & 0 & 1 & 0 & 0 & 0 & 0 & 0 & 0 & 0 \end{Bmatrix}^T.$$

Considering the boundary conditions, Eq. (15) is modified to

$$\left[\begin{array}{c|ccc} k_{22} & k_{24} & \cdots & k_{2,12} \\ \hline k_{42} & k_{44} & \cdots & k_{4,12} \\ \vdots & \vdots & \ddots & \vdots \\ k_{12,2} & k_{12,4} & \cdots & k_{12,12} \end{array}\right]\left\{\begin{array}{c} d_2 \\ \hline d_4 \\ \vdots \\ d_{12} \end{array}\right\} = \{0 \quad 0 \quad 1 \quad 0 \quad 0 \quad 0 \quad 0 \quad 0 \quad 0 \quad 0\}^T, \tag{17}$$

where k_{ij} is the element in the ith row and jth column of the matrix $\mathbf{K}^g$, and d_i is the element in the ith row of $\mathbf{D}^g$.

By solving Eq. (17), the displacement components of every node in global coordinate system can he determined, and then these displacement components in local coordinate systems of beams can be obtained using Eq. (11). The coefficient vector $\mathbf{C}^{(i)}$ can then be determined by Eq. (6), and substituting $\mathbf{C}^{(i)}$ into Eq. (4), the displacement components at any positions of the multi-beam frame model is obtained.

4 RESULTS AND DISCUSSION

The simplified 2.5D model developed in this paper has been used to carry out the frequency response analysis of a U-section viaduct, the cross section of which has been shown in Fig. 1 and has an area A = 2.1 m^2 and moment of inertia I = 0.82 m^4. The concrete used in the viaduct has a Young's modulus E = 3.62e10 Pa, and density ρ = 2500 kg/m^3. The length of the viaduct between two neighboring piers is L = 30 m. It is assumed that a 1 N/m of uniform harmonic load is acting on each rail.

The viaduct is divided into n sections along its longitudinal direction, and every section can be simplified into a multi-beam frame model, which consists of three beams having a rectangular cross section of height h = 0.24 m and width b = (L/n) m, and a lumped mass having a mass of m = ($0.12 \cdot b \cdot \rho$) kg and moment of inertia J = 49.561 kg•m^2.

Once the displacement frequency response of the viaduct is determined using the simplified 2.5D model, the vibrational energy of the viaduct is given by

$$E_{bridge}(\omega) = \sum_{j=1}^{n}\sum_{i=1}^{3}\left(b\int_0^{L_i}\left(\omega V_{i,j}(x_i)\right)^2 \mathrm{d}\,x_i\right), \tag{18}$$

where L_i is the length of beam i in the multi-beam frame model, i = 1, 2 and 3; and $V_{i,j}$ (x_i) is the normal displacement of beam i in the jth section of the viaduct.

The total energy, bottom plate energy and side plate energy of the simplified 2.5D model of the viaduct are shown in Fig.5. It is observed that the bottom plate has much greater contribution to the total energy than the side plate.

A FE model of the viaduct, which is composed of shell elements, is also developed using the ANSYS software and compared with the 2.5D model. The bottom plate energy of the longitudinal beam model, the simplified 2.5D model, and the FE shell model of the viaduct are compared in Fig. 6(a). And Fig. 6(b) and 6(c) shows the total energy of the latter two models and the relative error in dB between them, respectively. It is shown that the differences between the two models are about 2dB averaged in 1-10Hz, 9dB in 11-100Hz and 8dB in 101-500Hz. Moreover, the vibrational energy calculated from the simplified 2.5D model is lower than that from the FE model because the longitudinally and laterally coupled vibration modes of the viaduct structure are not concerned in the simplified 2.5D model.

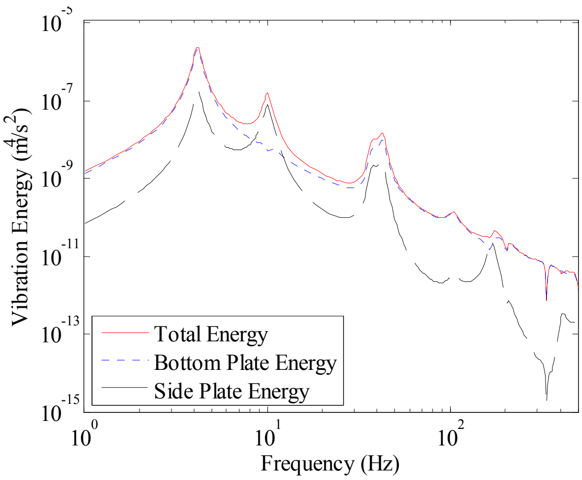

Figure 5: Energy of total, bottom plate and side plate of the simplified 2.5D model.

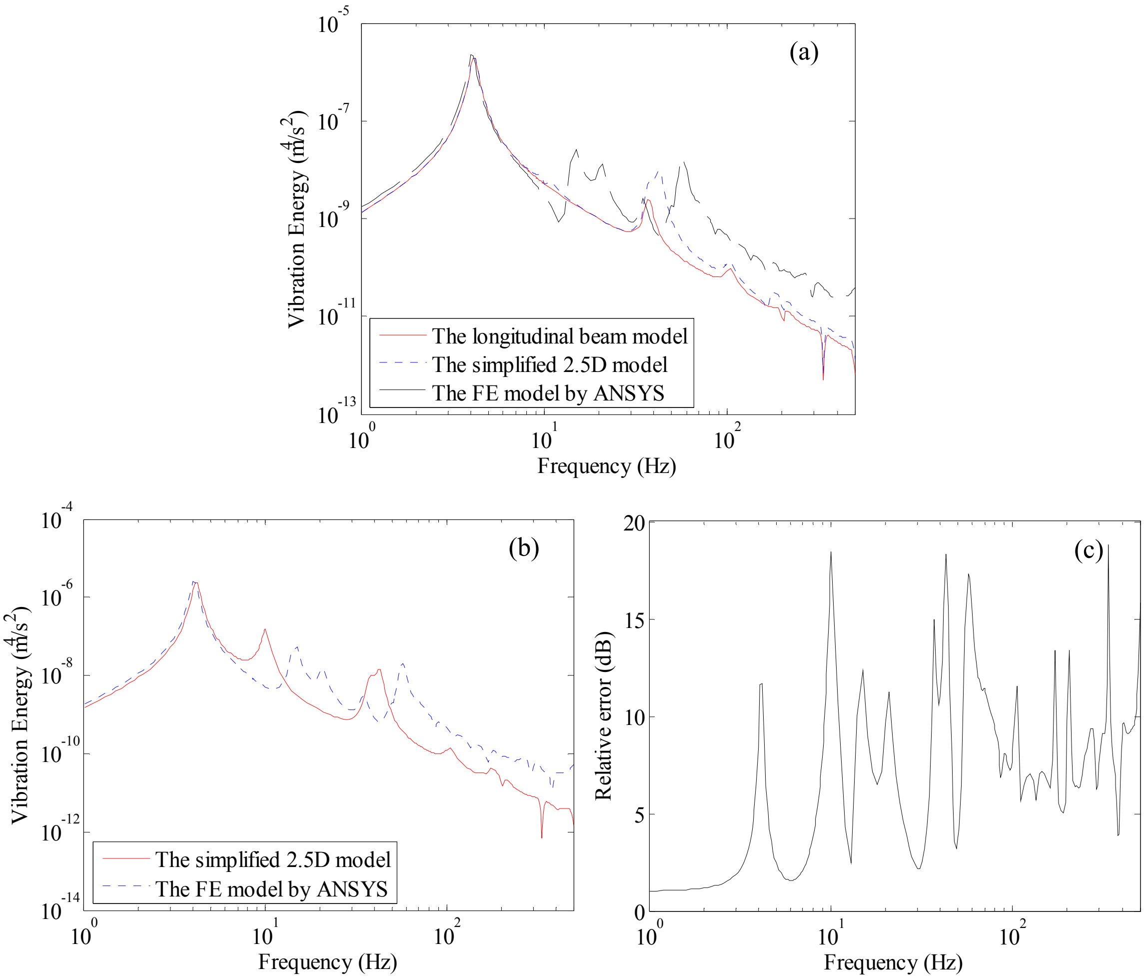

Figure 6: Comparison of the longitudinal beam model, the simplified 2.5D model and the FE model of the viaduct: (a) the bottom plate energy of the three models; (b) total energy of the latter two models; (c) relative error in dB of total energy of the latter two models.

5 CONCLUSION

A simplified 2.5D model is developed for the dynamic response analysis of a U-section viaduct under uniform harmonic excitation. A longitudinal beam model is used to simulate the vibration modes of the viaduct along the track, and a multi-beam frame model is used to simulate the dynamic properties of the cross section of the viaduct. The two models are combined by multiplying the displacement response distribution of the multi-beam frame model by an enlarging coefficient simultaneously. In doing so, the average displacement of a certain section can be obtained by the longitudinal beam model directly. Although the simplified beam model is not accurate enough for predicting the absolute response of the viaduct structure, it can effectively be used for performance comparison among the measures of vibration and noise control, as the system errors due to the incompleteness of the simplified model can be cancelled when carrying out comparisons. As the calculations by the simplified beam model are much easier, compared to the FE model, it is therefore suitable for quick prediction of the performances of the vibration and noise control measures.

REFERENCES

[1] Crockett, A. R. and Pyke, J. R. Viaduct design for minimization of direct and structure-radiated train noise. *J. Sound Vib*. (2000) **231**: 883-897.

[2] Wu, T. X. and Liu, J. H. Sound emission comparisons between the box-section and U-section concrete viaducts for elevated railway. *Noise Control Engr. J.* (2012) **60**: 450-457.

[3] Li, Q. and Wu, D. J. Analysis of the dominant vibration frequencies of rail bridges for structure-borne noise using a power flow method. *J. Sound Vib*. (2013) **332**: 4153-4163.